热烈庆祝中国地质学会成立100周年
1922～2022
www.geojournals.cn/georev

贵州纳雍营盘中二叠统茅口组硅质岩成因及其地质意义

杨贵园[1,2),高军波[1,2),杨瑞东[1,2),刘志臣[3),徐海[4)

1)贵州大学资源与环境工程学院,贵阳,550025;
2)贵州大学喀斯特地质资源与环境教育部重点实验室,贵阳,550025;
3)贵州省地质矿产勘查开发局一〇二地质大队,贵州遵义,563003;
4)铜仁学院旅游与地理系,贵州铜仁,554300

内容提要:二叠纪是地球演化历史进程中的重要一环,并在我国华南地区中二叠统茅口组(孤峰组)地层中普遍沉积一套层状硅质岩,它们可能与中、晚二叠世系列重大地质事件之间有着密切的成因联系。笔者等以位于扬子地块西南缘的贵州纳雍营盘茅口组硅质岩作为研究对象,通过对硅质岩元素地球化学组成进行研究发现,硅质岩Al/(A1+Fe+Mn)值以及多项成因判别图解等指示其形成过程中有明显的热水物质输入,具有热水成因硅质岩的特征。结合区域古地理特征,以及硅质岩 Ce/Ce^{*}、$(La/Ce)_{N}$ 值等综合分析,认为硅质岩形成于黔中台沟内的深水环境。综合考虑区域范围内中二叠世硅质岩研究成果,并分析纳雍营盘硅质岩与峨眉山玄武岩空间关系及峨眉地幔柱活动历史,认为峨眉地幔柱早期海底火山活动可能对包括营盘在内的华南地区中二叠世晚期硅质岩沉积具有重要控制作用。

关键词:成因;硅质岩;二叠纪;纳雍营盘;贵州

晚古生代末期,全球古构造—岩浆活动及古地理演化经历了重大变革,早二叠世冰室消融造成了华南板块广泛区域发育浅水碳酸盐台地的沉积,而中—晚二叠世峨眉地幔柱的隆升引起区域上强烈的拉张构造及岩浆—热液活动,不仅形成了大面积峨眉山玄武岩堆积,而且发育广泛的岩浆—热液及沉积成矿事件(张成江等,1999;何斌等,2006;Shellnutt et al.,2009;徐义刚等,2013a)。受地壳拉张运动及深大断裂强烈活动的影响,扬子板块西缘浅水碳酸盐台地发生强烈的沉降分异从而形成黔北—滇东一带裂谷盆地(即黔中台沟),并在台沟内部广泛发育一套特殊的硅质岩建造,与晚古生代末期全球性硅质沉积事件相对应(Murchey et al.,1992;周永章等,2004;Kametaka et al.,2005;邱振等,2010;加娜提古丽·吾斯曼等,2017;叶远谋等,2020;赵振洋等,2020)。前人对华南二叠纪硅质岩研究已积累有丰硕成果,但有关硅质岩的成因类型认识不一,存在有热水成因(夏邦栋等,1995;杨玉卿等,1997;周永章等,2004;林良彪等,2010;叶远谋等,2020)和生物成因(王忠诚等,1995;Kametaka et al.,2005;杨水源等,2008)的争论。最近,赵振洋等(2020)对中下扬子区北缘中二叠统孤峰组硅质岩进行研究,推测它们的形成可能与峨眉地山玄武岩早期海底喷发作用有关。

位于滇东、黔北一带黔中台沟内的二叠纪沉积锰矿床赋矿围岩主要以硅质岩、硅质灰岩、灰岩等为主。前人研究已证实,黔中台沟内的硅质建造与锰矿床在成因上具有紧密联系(刘志臣等,2013;江冉等,2016;徐海等,2017)。特别是处于黔中台沟东缘的遵义二叠纪锰矿底部分布有一套特殊的硅质岩、硅化灰岩,发育有条带状、角砾状结构(刘志臣等,2013),前人将其称之为"白泥塘层"。我们最

注:本文为国家自然科学基金资助项目(编号:42163006,41890841,U1812402)、贵州省沉积矿床科技创新人才团队项目(编号:黔科合平台人才[2018]5613)、贵州省人才基地项目(编号:RCJD2018-21)和贵州省研究生科研基金立项项目(编号:黔教合YJSCXJH[2020]181)的成果。
收稿日期:2022-03-21;改回日期:2022-06-22;网络首发:2022-07-20;责任编辑:刘志强。Doi:10.16509/j.georeview.2022.07.031
作者简介:杨贵园,女,1997年生,硕士研究生,沉积矿床专业;Emali:yangguiyuan_08@163.com。通讯作者:高军波,男,1985年生,博士,教授,硕士生导师,主要从事沉积矿床研究和教学;Email:gaojunbo1985@126.com。

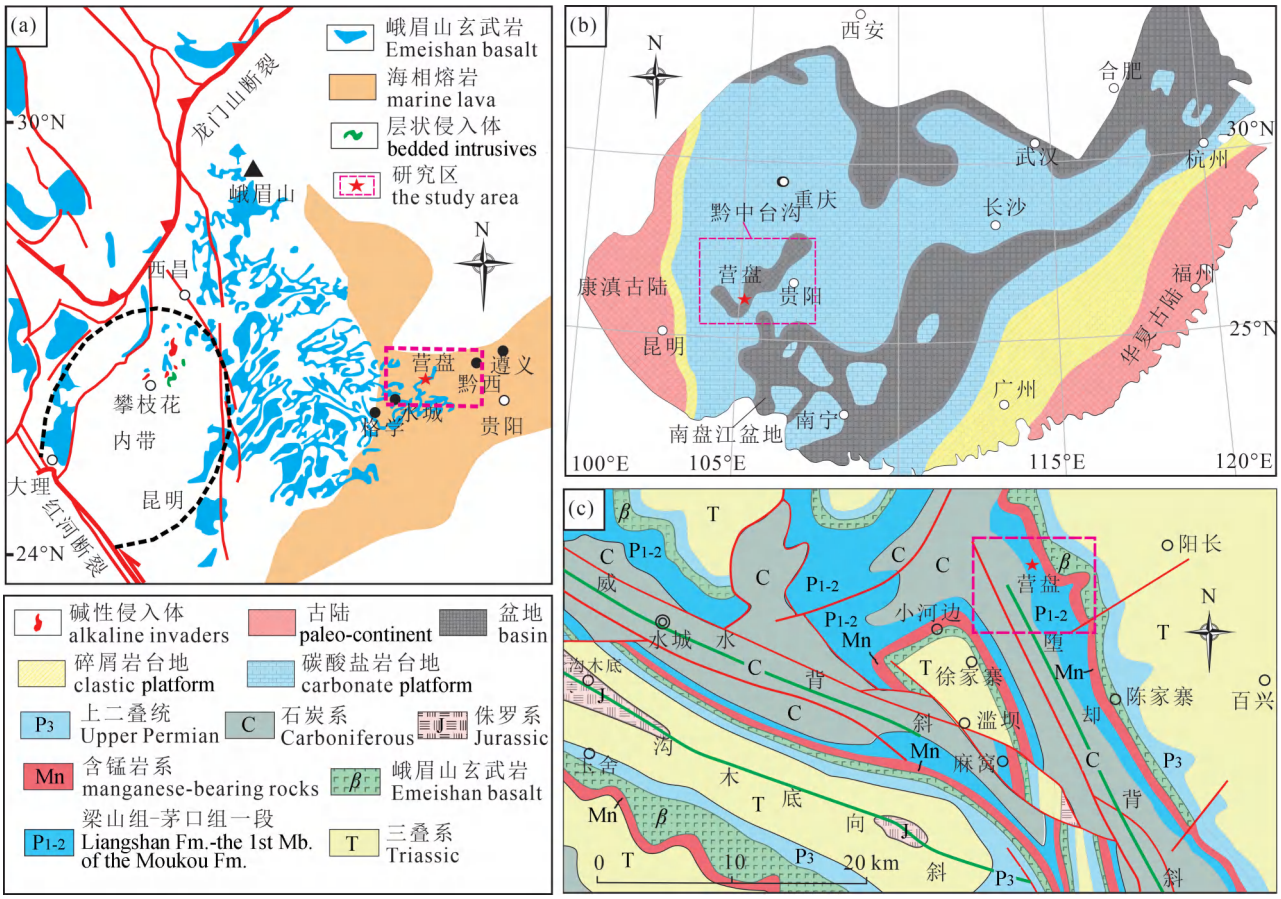


图 1 华南东南部地质背景与贵州省水城—纳雍地区地质概况略图

Fig. 1 The sketch of the geological setting of southeastern China and the geological profile of the Shuicheng—Nayong region of Guizhou Province

(a)华南峨眉山大火成岩省分布图(据 Ukstins-Peate et al., 2008);(b)华南板块瓜德鲁普世晚期岩相古地理图(据 Wei Hengye et al., 2016);(c)纳雍营盘剖面地质简图(据刘平等, 2008)

(a) Distribution map of Emeishan Igneous Province in south China (from Ukstin-Peate et al., 2008); (b) lithofacies palaeogeography of the Late Guadalupian in South China Plate (from Wei Hengye et al., 2016); (c) profile geological sketch of Yingpan, Nayong (from Liu Ping et al., 2008)

近的调查工作表明,位于黔中台沟西南缘的水城—纳雍一带在中、晚二叠世沉积有连续的硅质岩、灰岩、含锰灰岩建造,且硅质岩常与锰矿互层产出。该区更靠近峨眉地幔柱及玄武岩分布区,且与硅质岩紧密共生产出许多锰矿床,但以往研究对此关注较少,区内硅质岩沉积过程中记录有哪些与峨眉地幔柱、锰矿成矿等重要地质事件有关的信息,值得深入挖掘。

为此,笔者等以纳雍营盘中二叠统茅口组硅质岩为主要研究对象,在详细地野外调查工作基础之上,重点利用元素地球方法探讨硅质岩的成因,限定硅的来源,并试图阐释硅质岩成岩过程与区域构造事件、古地理变迁、二叠纪锰矿成矿作用等重要地质事件之间的关系。

1 地质背景

二叠纪时期,全球范围内发生了一系列重大地质历史事件。早二叠世冈瓦纳大陆冰川大规模消融,导致全球海平面普遍上升,形成大规模海侵作用(Montañez et al., 2013; Qie Wenkun et al., 2019),并造成我国西南地区发育大面积浅水碳酸盐岩台地(颜佳新等, 2002)。中—晚二叠世,峨眉地幔柱强烈活动引发峨眉地裂运动(陈文一等, 2003),巨量基性岩浆喷出/溢出地表,并形成了体积庞大的峨眉山玄武岩(图 1a)(Hou Zengqian et al., 2006; 徐义刚等, 2013b),并因应力释放不均造成地壳差异性升降(He Bin et al., 2003),导致碳酸盐台地发生强烈分异,并在云南宣威,后经贵州水城、黔西直抵遵

义一带形成一条宽约 25~35 km、长约 300 km 的深水台沟,即“黔中台沟”(图 1b)(陈文一等, 2003)。滇东、黔北二叠纪锰矿均分布于黔中台沟内,并限制于台沟相硅质岩、硅质泥岩、生物碎屑灰岩建造中(刘平等, 2008)。纳雍营盘锰矿主要位于黔中台沟西南缘,是我国南方二叠纪锰矿床的重要组成部分,围岩以硅质岩、含锰灰岩等为主。从地理位置来看,纳雍营盘位于峨眉山大火成岩省东部(图 1a),而且营盘剖面沉积连续,特别是发育有大量硅质岩沉积,它们很可能详细记录着与峨眉山大火成岩省有关的热水活动等在黔中台沟内的发展演化历史。从纳雍营盘地区地质概况来看,区内主要发育有 NW 向的百兴向斜和威水背斜,以及 NNW 向的堕却背斜和 NWW 向的沟木底向斜。纳雍营盘剖面主要位于堕却背斜的东翼(图 1c)。

中二叠世晚期,峨眉地慢柱活动引发了强烈的岩浆活动,形成了著名的峨眉山大火成岩省。峨眉山大火成岩省主要由玄武岩、镁铁—超镁铁质层状岩体、碱性杂岩体、酸性岩等组成(徐义刚等, 2013a),其空间分布跨越了云南、四川和贵州三省,出露面积约为 2.5×10^5 km^2(徐义刚等, 2013b)。关于峨眉地幔柱活动历史,大量的年代学研究表明,峨眉山玄武岩主喷发期很可能在~260 Ma(Zhou Meifu et al., 2002; He Bin et al., 2007; Zhong Hong et al., 2011)。而与峨眉山大火成岩省相关的酸性火山活动似乎持续的时间更长,甚至可延续至~257 Ma(Zhong Yuting et al., 2020; Shellnutt et al., 2020)。实际上,在大规模峨眉山玄武岩形成之前,可能还存在有较大规模的水下火山喷发活动,并在云南丽江、昆明,以及贵州盘县、普安等地区形成了大量的火山灰、火山角砾岩等(Wignall et al., 2009; Sun Yadong et al., 2010; 朱江, 2019, Yan Hao et al., 2020)。朱江(2019)研究认为,峨眉山地幔柱最早喷发时间很可能在~262 Ma。古生物学及地层学研究也发现,地幔柱早期喷发时间大致对应于 Capitanian 中期的 *Jinogondolella altudaensis* 带(~263 Ma)(孙亚东, 2013),这些研究工作对于更好地约束峨眉地幔柱早期火山活动的启动时间均有重要参考价值。

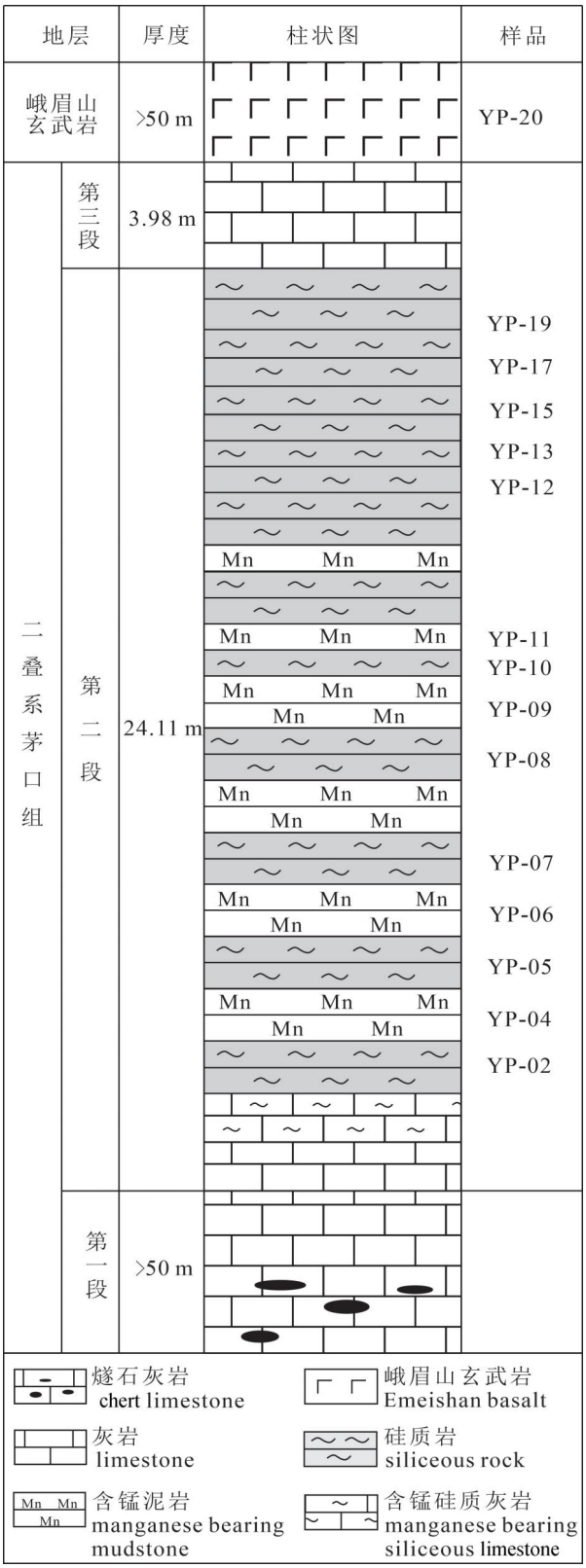


图 2 黔中台沟西南缘纳雍营盘中二叠统茅口组地层岩性柱状图

Fig. 2 Lithologic column of the Middle Permian Maokou Formation at Yingpan, Nayong, southwestern margin of the Qianzhong Trench

2　剖面位置和样品特征剖面沉积序列

2.1　剖面沉积序列

纳雍营盘剖面沉积连续且较为完整,发育有硅质岩、含锰硅质岩、含锰硅质灰岩和氧化锰(图 2)。

野外观察可见氧化锰矿层与硅质岩、含锰灰岩等互层,土状氧化锰多分布于地表浅部,并与极薄硅质岩互层,由地表向深部延伸,逐渐过渡为含锰硅质灰岩、含锰硅质岩和硅质岩。

剖面自上而下,岩性特征依次为:

峨眉山玄武岩组:

为绿灰、黑灰色块状拉斑玄武岩,风化后呈黄、褐黄色松散砂状玄武岩 厚度大于 50 m

----------假整合接触----------

中二叠统茅口组:

第三段:灰、浅灰色中厚层灰岩、生物碎屑灰岩等 厚 3.98 m

第二段:为一套含锰硅质灰岩、含硅质灰岩、硅质岩、生物碎屑灰岩等,岩石氧化后表面有土状氧化锰分布

该段顶部以深灰色硅质灰岩、含硅质灰岩,时夹少量深灰色生物碎屑灰岩 厚 5.25 m

中部为棕黑色"土状"氧化锰矿层,往内过渡为黑色"碴状"氧化锰矿层夹硅质岩,深部则为硅质灰岩和含锰硅质灰岩,横向上表现为氧化锰与含锰硅质灰岩互层 厚 14.30 m

底部主要为灰、深灰色含锰条带硅质灰岩、硅质条带硅化灰岩 厚 4.56 m

第一段:以灰、浅灰色厚层—块状生物碎屑灰岩,中厚层—厚层燧石灰岩 厚 >50 m

2.2 矿物组构

纳雍营盘剖面硅质岩主要呈层状、条带状产出,在剖面中部条带状硅质岩中夹有薄层含锰泥岩(图 3a),上部主要为灰黑色薄层条带状含锰硅质岩及硅质岩(图 3b)。显微镜下观察,含锰硅质岩中可见锰质及铁质条带呈不规律的纹层状产出(图 3c),硅质岩物质组成以大量细粒石英矿物为主,粒间分布粘土矿物(图 3d)。

3 分析测试方法与结果

3.1 样品采集及测试方法

在纳雍营盘剖面共采集 11 件样品,其中硅质岩、含锰硅质岩 10 件,峨眉山玄武岩 1 件。样品主量元素分析在广州澳实分析检测中心完成,测试方法详见徐海(2022)。微量及稀土元素测试在中国科学院地球化学研究所矿床地球化学国家重点实验室完成。样品测试过程为:将样品粉碎研磨至 200 目,然后称取 50 mg 粉末置于聚四氟乙烯坩埚中并加入 HF 和 HNO_3 混合溶液加热消解,待消解完成后进行干燥、定容及再溶解等步骤后,采用等离子质谱仪(ICP-MS)进行测定。详细测试方法见 Qi Liang 等(2000)。

3.2 分析测试结果

纳雍营盘硅质岩 Al_2O_3 含量介于 0.15%~0.27%,含锰硅质岩 Al_2O_3 含量介于 0.15%~0.25%,而玄武岩样品(YP-20)的 Al_2O_3 含量较高,为 12.4%。硅质岩 SiO_2 含量介于 93.4%~96.03%,含锰硅质岩 SiO_2 含量介于 82.71%~94.44%,玄武岩 SiO_2 含量为 49.96%。硅质岩中 TiO_2 含量普遍小于 0.01%,玄武岩中则相对较高,达到 4.16%,总体归属高钛玄武岩系列(Xu Yigang et al., 2001)。纳雍营盘硅质岩相对富集 As、Co、Cu、Ni、U、V、Zn、Sr、Sb、Mo,贫 Ba、Ca、Ag、Th 等元素。

纳雍营盘硅质岩及含锰硅质岩的稀土元素(REE)总量较低,介于 15.4×10^{-6}~68.6×10^{-6},平均值为 30.9×10^{-6}。玄武岩稀土总量相比较高,为 268×10^{-6}。其 LREE/HREE 比值介于 4.21~6.49,平均值为 5.7,且具有明显 Ce 负异常(Ce/Ce^* = 0.22~0.63)、Eu 弱正异常(Eu/Eu^* = 0.82~1.14)以及明显 Y 的正异常。另外,硅质岩及含锰硅质岩 Y/Ho 值介于 34.5~55.8,平均值为 47.4。

4 讨论

4.1 硅质岩成因分析

通常,硅质岩中 Fe、Mn 富集与热水物质贡献有关,Al 含量则可约束陆源物质的输入程度,因此 Al/(Al+Fe+Mn)值可以作为判断热水组份参与沉积作用的指标(Boström et al., 1969)。其中,典型热水沉积物的 Al/(Al+Fe+Mn)<0.35(Boström, 1983)。纳雍营盘硅质岩的 Al/(Al+Fe+Mn)值为 0.01~0.08,远小于 0.35,显示热水活动的积极贡献。

Al—Fe—Mn 及 Fe—Mn—(Cu+Ni+Co)三角图解对于分析硅质岩成因有重要指示意义(Adachi et al., 1986; Boström, 1983)。在 Al—Fe—Mn 和 Fe—Mn—(Cu+Ni+Co)图解中(图 4a、b),硅质岩总体落在热水沉积区及其附近,表明硅质岩的形成与热液活动有关,其硅源很可能来自于热液体系。SiO_2 和 Al_2O_3 比值也可有效判断硅质岩的成因(Wonder et al., 1988),纳雍营盘硅质岩在 SiO_2—Al_2O_3 成因判别图中主要落入热水沉积区(图 4c)。在 U—Th 相关性图解中(图 4d),也显示相类似的特征。这些地球化学特征均表明,纳雍营盘硅质岩形成过程中很可能有明显的热水活动参与,指示硅更多地来自于热水体系。

纳雍营盘硅质岩及含锰硅质岩 REE 总量低,



图 3 黔中台沟西南缘纳雍营盘中二叠统茅口组地层及样品电子显微镜照片

Fig. 3 Specimen and electron microscope images of Middle Permian Maokou Formation at Yingpan, Nayong, southwestern margin of the Qianzhong Trench

(a) 硅质岩与氧化锰矿互层; (b) 层状硅质岩野外特征; (c) 锰质条带与铁质条带互层; (d) 球粒状石英与有机质紧密共生

(a) Siliceous rock interbedded with manganese oxide ore; (b) field characteristics of layered siliceous rocks; (c) interbedded Mn and Fe bands; (d) nodular quartz is closely symbiotic with organic matter

LREE/HREE 值均大于 1,且具有明显 Ce 负异常和 Y 正异常(图 5),符合典型热水沉积硅质岩特征。正常海相沉积物 Y/Ho 平均值为 55,而陆源物质、球粒陨石、火山岩的 Y/Ho 平均值为 28(Nozaki et al., 1997)。Y/Ho 值介于 34.5 ~ 55.8,高于陆源物质、球粒陨石及火山岩而接近于海水的 Y/Ho 值,结合前述地球化学指标,说明纳雍营盘硅质岩属于热水沉积且受陆源物质影响小,而相比海水营盘硅质岩 Y/Ho 值较低的原因可能是受到火山热液作用影响。

4.2　硅质岩沉积环境

Al_2O_3 及 TiO_2 含量主要来自陆源物质输入,因

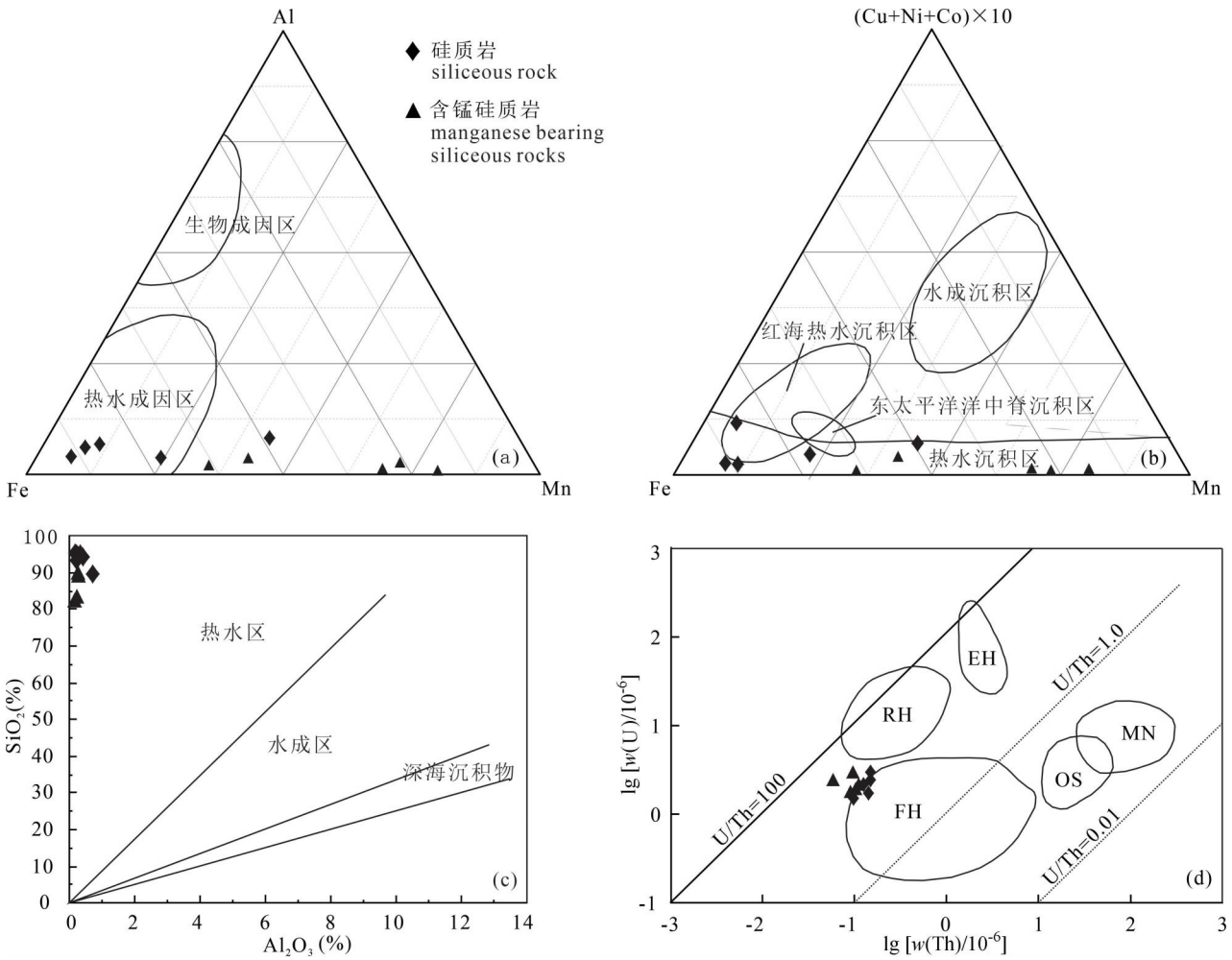


图 4 黔中台沟西南缘纳雍营盘中二叠统茅口组硅质岩成因判别图解

Fig. 4 Genetic discrimination diagram of the siliciclastic rocks of the Middle Permian Maokou Formation at Yingpan, Nayong, southwestern margin of the Qianzhong Trench

(a) Fe—Mn—Al 成因判别图解(据 Adachi et al., 1986); (b) Fe—Mn—(Cu+Ni+Co)图解(据 Boström, 1983); (c) SiO_2—Al_2O_3 成因判别图解(底图据 Wonder et al., 1988); (d) U—Th 关系图(据 Boström, 1983)。EH—东太平洋隆起热水沉积区; RH—红海热卤水沉积区; FH—古热液沉积区; OS—正常远洋沉积区; MN—锰结核沉积区

(a) Genetic discrimination diagram of Fe—Mn—Al (after Adachi, 1986); (b) Fe—Mn—(Cu+Ni+Co) diagram (after Bostrom, 1983); (c) SiO_2—Al_2O_3 genetic discrimination diagram (after Wonder et al., 1988); (d) U—Th diagram (after Boström, 1983). RH—Red Sea hydrothermal district; EH—East Pacific hydrothermal district; FH—Fe—Mn paleo-hydrothermal district; OS—ocean sediment district; MN—manganese district; AH—alumina sediment district

此其含量可用于指示硅质岩沉积环境。纳雍营盘剖面主量元素含量检测显示(表 1),样品 Al_2O_3 和 TiO_2 含量极低,硅质岩及含锰硅质岩 Al_2O_3 含量范围在 0.05%~0.25%,平均为 0.2%,TiO_2 含量均低于能被检测值,说明了其成矿物质来源并非陆源输入。

Ce 异常值能够有效约束硅质岩的形成环境(表 2),其中大洋中脊附近硅质岩的 Ce/Ce^* 值约为 0.29,远洋盆地硅质岩 Ce/Ce^* 值约为 0.55,大陆边缘形成的硅质岩 Ce/Ce^* 值为 0.90~1.30(Murray et al., 1991)。纳雍营盘二叠系茅口组硅质岩 Ce/Ce^* 值介于 0.22~0.63,显示硅质岩沉积环境介于洋中脊附近和远洋盆地环境,结合纳雍营盘二叠纪时期地质背景和岩相古地理特征,Ce/Ce^* 值其实质反映了硅质岩主要形成于受同沉积断裂控制的黔中台沟内。

$(La/Ce)_N$ 值是判别硅质岩沉积环境的重要指标,其中大陆边缘区域沉积硅质岩 $(La/Ce)_N$ = 0.5~1.5,远洋盆地内硅质岩 $(La/Ce)_N$ = 1~2.5,大洋中脊附近硅质岩 $(La/Ce)_N \geq 3.5$(Murray, 1994)。纳

表 1 黔中台沟西南缘纳雍营盘中二叠统茅口组硅质岩主量元素(%)分析结果

Table 1 Analysis results of main elements (%) of the siliciclastic rocks of the Middle Permian Maokou Formation at Yingpan, Nayong, southwestern margin of the Qianzhong Trench

样号	岩性	Al_2O_3	CaO	TFe_2O_3	K_2O	MgO	Mn	Na_2O	P_2O_5	SiO_2	TiO_2	烧失	Mn/Fe	$\frac{Al}{(Al+Fe+Mn)}$
YP-20	峨眉山玄武岩	12.40	5.06	15.16	2.81	3.68	0.12	2.71	0.49	49.96	4.16	2.85	0.01	0.38
YP-19	硅质岩	0.15	0.43	1.60	0.03	0.02	0.11	<0.01	0.02	96.03	<0.01	0.95	0.10	0.06
YP-17	硅质岩	0.19	0.48	1.64	0.04	<0.01	0.15	0.01	0.03	95.49	<0.01	1.02	0.13	0.07
YP-15	硅质岩	0.21	0.15	3.00	0.06	<0.01	0.71	<0.01	0.05	93.40	<0.01	1.11	0.34	0.04
YP-13	硅质岩	0.17	0.16	2.84	0.03	<0.01	0.15	<0.01	0.02	94.80	<0.01	1.18	0.08	0.04
YP-12	硅质岩	0.27	0.21	1.19	0.06	<0.01	0.74	<0.01	0.01	95.27	<0.01	1.51	0.89	0.08
YP-10	含锰硅质岩	0.15	0.27	2.49	0.26	0.19	7.14	<0.01	0.07	82.71	<0.01	3.38	4.10	0.01
YP-08	含锰硅质岩	0.23	0.20	3.88	0.15	0.13	6.22	<0.01	0.11	83.57	<0.01	3.17	2.29	0.01
YP-07	含锰硅质岩	0.19	0.10	2.29	0.04	<0.01	1.22	<0.01	0.03	94.44	<0.01	1.06	0.76	0.03
YP-05	含锰硅质岩	0.22	0.13	5.19	0.05	0.02	1.98	<0.01	0.06	89.73	<0.01	1.73	0.55	0.02
YP-02	含锰硅质岩	0.25	0.30	2.14	0.12	0.09	4.14	<0.01	0.03	89.38	<0.01	2.39	2.76	0.02

注:数据引自徐海(2022)。

表 2 黔中台沟西南缘纳雍营盘中二叠统茅口组硅质岩微量和稀土元素分析结果($\times10^{-6}$)及参数特征

Table 2 Analysis results of trace and rare earth elements ($\times10^{-6}$) and parameter characteristics of the siliciclastic rocks of the Middle Permian Maokou Formation at Yingpan, Nayong, southwestern margin of the Qianzhong Trench

元素	YP-02	YP-05	YP-07	YP-08	YP-10	YP-12	YP-13	YP-15	YP-17	YP-19	YP-20
Li	1.85	0.945	0.805	1.42	1.375	1.53	1.44	1.34	1.59	1.41	11.1
Sc	0.535	0.285	0.249	0.456	0.423	0.371	0.34	0.476	0.362	0.286	22.6
V	108	79	31.4	105	108	111	109	106	86.2	73	346
Cr	111	123	55.5	79	60.5	203	106	103	131	93	35.8
Co	32.1	24.3	12	9.75	13.8	7.05	8.46	9.98	5.98	5.1	38.0
Ni	95.5	86	45	96	101	45	25.4	36.6	24.4	19.4	44.9
Cu	8.15	6.4	3.745	4.82	6.75	7.9	6.48	6.64	7.86	7.2	203
Zn	18.1	19.1	8.5	38.5	26.6	48	38.8	13.3	26.2	23.4	133
Ga	4.69	2.5	1.61	6.45	7.15	1.32	0.558	1.17	0.606	0.49	24.9
Ge	0.373	0.225	0.142	0.171	0.136	0.128	0.154	0.152	0.141	0.12	1.56
Sr	105	61	41.9	120	160	44.7	23.6	40.8	45.8	46.4	208
Zr	10.8	8.85	3.94	5.9	6.9	5.15	5.64	9.06	7.9	6.14	352
Nb	1.58	1.12	0.491	0.875	0.995	0.54	0.59	1.44	1.09	0.918	43.5
Mo	4.98	5	4.94	6	4.04	10.6	7.02	5.48	9.36	7.56	2.31
Ag	0.051	0.017	0.008	0.015	0.029	0.011	0.017	0.069	0.034	0.028	0.606
Cd	0.235	0.074	0.068	0.339	0.249	0.79	0.536	0.312	0.206	0.165	0.184
In	0.007	0.004	0.003	0.003	0.003	0.003	0.005	0.007	0.005	0.006	0.104
Sn	0.077	0.103	0.059	0.06	0.152	0.004	0.082	0.106	0.282	0.304	2.73
Sb	2.65	7	3.71	20.1	8.5	2.2	2.6	3.6	1.64	0.87	0.197
Ba	92	22.6	25.3	53.5	97.5	57	10.4	26.8	15.4	13.8	492
Hf	0.201	0.171	0.067	0.126	0.122	0.165	0.141	0.296	0.158	0.138	9.73
Ta	0.021	0.015	0.007	0.016	0.012	0.021	0.015	0.025	0.016	0.014	3.03
Tl	1.41	0.635	0.385	3.23	0.595	2.63	0.582	2.08	1.41	0.992	0.231
Pb	1.13	1.11	0.665	0.93	0.88	1.32	1.4	1.67	0.934	0.808	12.8
Th	0.097	0.091	0.059	0.126	0.104	0.15	0.112	0.15	0.139	0.098	7.32
U	2.99	1.8	2.45	2.16	1.94	2.98	2.18	2.44	1.72	1.51	1.69
La	16.6	4.84	4.28	13.6	9.65	13.2	5.86	10.4	8.82	7.5	44.6
Ce	15.1	4.96	4.12	11.8	5.4	4.67	6.44	7.56	6.08	4.5	99.5
Pr	3.35	0.62	0.675	1.68	1.59	1.67	0.916	1.45	1.18	0.92	13.9
Nd	16.2	2.83	3.18	7.5	7.4	7.65	4.04	6.24	5.3	4.02	62.1
Sm	3.3	0.58	0.64	1.38	1.52	1.37	0.78	1.23	0.94	0.712	13.2
Eu	0.88	0.142	0.162	0.324	0.401	0.341	0.154	0.28	0.234	0.168	3.76
Gd	4.24	0.74	0.785	1.88	1.75	1.82	0.96	1.55	1.29	0.964	11.3

元素	YP-02	YP-05	YP-07	YP-08	YP-10	YP-12	YP-13	YP-15	YP-17	YP-19	YP-20
Tb	0.595	0.106	0.108	0.261	0.25	0.239	0.14	0.224	0.175	0.13	1.61
Dy	3.58	0.66	0.64	1.6	1.49	1.47	0.882	1.44	1.07	0.794	8.67
Ho	0.76	0.143	0.128	0.328	0.304	0.323	0.188	0.316	0.228	0.17	1.59
Er	2.01	0.387	0.334	0.815	0.805	0.84	0.502	0.856	0.586	0.442	4.03
Tm	0.267	0.054	0.043	0.102	0.107	0.112	0.068	0.12	0.074	0.056	0.524
Yb	1.5	0.336	0.245	0.535	0.63	0.66	0.408	0.74	0.402	0.31	3.18
Lu	0.218	0.045	0.036	0.072	0.089	0.095	0.056	0.098	0.059	0.043	0.454
Y	30.3	7.6	6.8	14.6	13.7	17.2	6.48	13.5	11.9	9.48	38.7
Eu/Eu^*	1.08	1.00	1.06	0.92	1.14	0.99	0.82	0.94	0.97	0.93	1.45
Ce/Ce^*	0.47	0.63	0.55	0.54	0.31	0.22	0.63	0.44	0.42	0.38	0.91
ΣREE	68.60	16.44	15.38	41.88	31.39	34.46	21.39	32.50	26.44	20.73	268.42
LREE/HREE	4.21	5.65	5.63	6.49	4.79	5.20	5.68	5.08	5.81	6.13	7.56
$(La/Ce)_N$	2.29	2.03	2.16	2.40	3.72	5.89	1.90	2.87	3.02	3.47	0.93
Y/Ho	39.87	53.15	53.13	44.51	45.07	53.25	34.47	42.72	52.19	55.76	24.34

注:$Ce/Ce^* = 2\times Ce_N/(La_N+Pr_N)$,$Eu/Eu^* = 2\times Eu_N/(Sm_N+Gd_N)$;N 表示澳大利亚后太古代平均页岩(PAAS)(Mclennan, 1989)标准化比值。

雍营盘二叠纪硅质岩$(La/Ce)_N$值介于 1.9~5.89,平均为 2.98,结果显示硅质岩沉积环境贴近于大洋中脊。在 Fe_2O_3/TiO_2—$Al_2O_3/(Al_2O_3+Fe_2O_3)$、$(La/Ce)_N$—$Al_2O_3/(Al_2O_3+Fe_2O_3)$图解中(图 6),投图结果同样显示硅质岩样品均分布于大洋中脊区域内及附近区域。强烈的热液活动是图解中指示洋中脊沉积区的根本原因,然而除洋中脊以外,海底深大断裂、弧后盆地、裂谷、岛弧等地质构造背景同样可以广泛发育热液活动(Adachi et al., 1986; Yamamoto, 1987; 张聪等, 2017)。事实上,中二叠世茅口期研究区并不存在洋中脊,主要是在东西向展布的黔中台沟分布规模不等的同沉积断裂,并伴随有较为广泛的热水沉积事件,因此图中显示出同样具有热液发育背景的洋中脊沉积区。所以,纳雍营盘硅质岩$(La/Ce)_N$比值、Fe_2O_3/TiO_2—$Al_2O_3/(Al_2O_3+Fe_2O_3)$及$(La/Ce)_N$—$Al_2O_3/(Al_2O_3+Fe_2O_3)$图解实质上反映硅质岩成岩过程主要受控于黔中台沟内热液体系控制。

4.3 成因意义探讨

华南二叠纪时期发育大面积的硅质岩沉积,但有关硅源及其形成环境复杂多样。其中滇东、黔北地区黔中台沟内发育的硅质岩是华南二叠纪大面积硅质沉积事件的重要组成部分。近年来,针对黔中台沟东缘遵义地区锰矿底板硅质岩研究,结果均指示其属于热水沉积成因(刘志臣等, 2013; 江冉等, 2016; 徐海等, 2017),而且在与硅质岩具有紧密成因关系的二叠纪锰矿床中揭露出与峨眉地幔柱有关的热水/液活动的地质信息(Gao Yongbao et al., 2018; Xu Hai et al., 2021)。大量调查研究结果已表明,与峨眉地幔柱有关的火山活动很可能经历了至少两个大的时期(陈文一等, 2003; Sun Yadong et al., 2010; 朱江, 2019)。在地幔柱活动形成大规

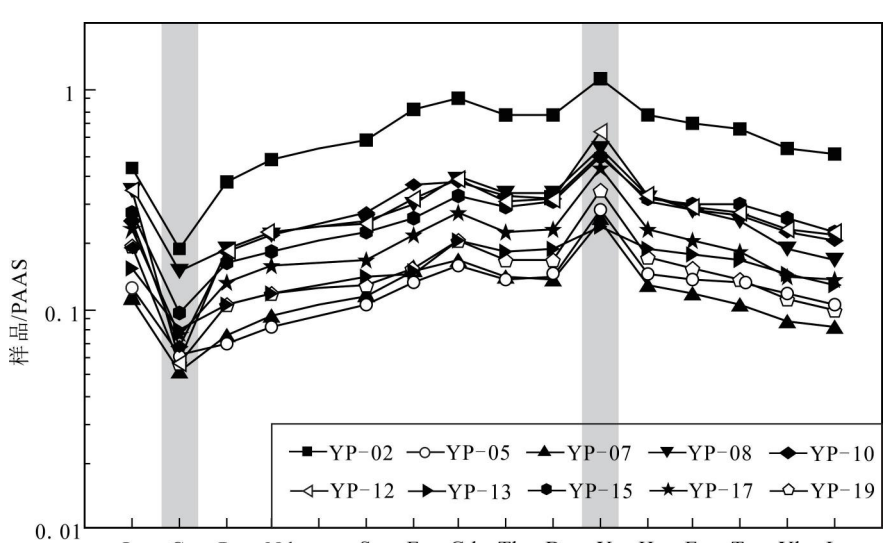


图 5 黔中台沟西南缘纳雍营盘中二叠统茅口组硅质岩稀土元素标准化配分模式图[标准化值——澳大利亚后太古代平均页岩(PAAS)——据 Mclennan, 1989]

Fig. 5 Normalized distribution patterns of the rare earth elements in the siliciclastic rocks of the Middle Permian Maokou Formation at Yingpan, Nayong, southwestern margin of the Qianzhong Trench (the value for normalization of the Australian Post-Archean mean Shale (PAAS) from Mclennan, 1989)

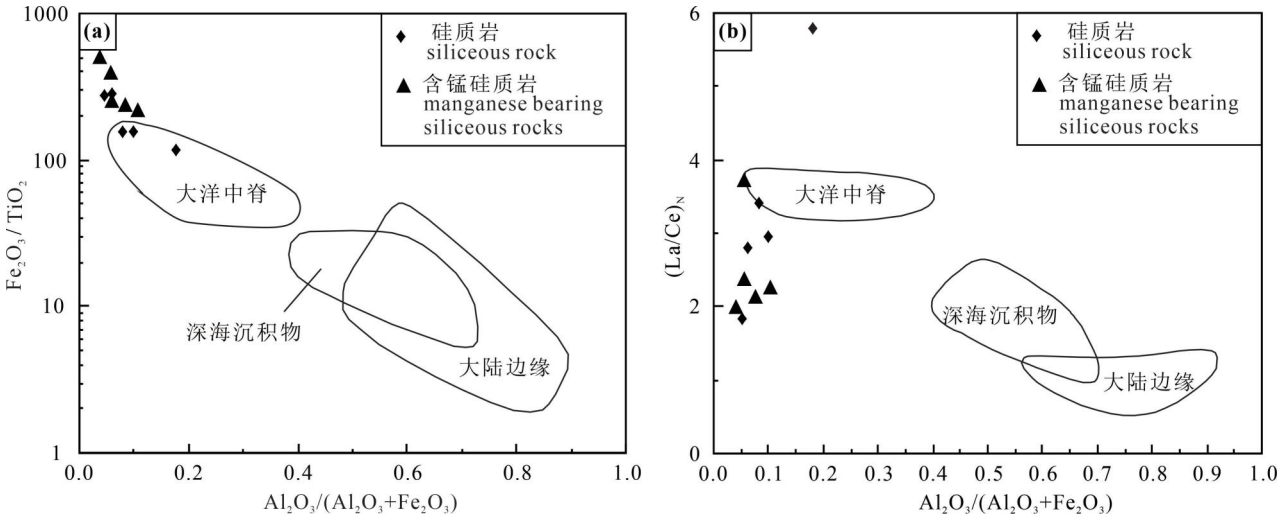


图 6 硅质岩 (a)Fe_2O_3/TiO_2—$Al_2O_3/(Al_2O_3+Fe_2O_3)$辨别图解(据 Murray, 1994)
和(b)$(La/Ce)_N$—$Al_2O_3/(Al_2O_3+Fe_2O_3)$辨别图解(据 Murray, 1994)

Fig. 6 (a) Fe_2O_3/TiO_2—$Al_2O_3/(Al_2O_3+Fe_2O_3)$ discrimination diagram (after Murray, 1994) and (b) $(La/Ce)_N$—$Al_2O_3/(Al_2O_3+Fe_2O_3)$ discrimination diagram (after Murray, 1994) of siliceous rock

模溢流玄武岩及相伴的侵入岩(Xu Yigang et al., 2001; Zhong Hong et al., 2009)之前,还存在一段时期相对剧烈的火山活动,其发生时间大致对应于 Capitanian 中期的 *Jinogondolella altudaensis* 带(~260 Ma)(Wu Qiong et al., 2020),而且显示海底/水下喷发特征,形成的火山碎屑物质可以从云南宾川一直延伸到贵州水城、纳雍、织金等地(Wignall et al., 2009; Sun Yadong et al., 2010; 朱江, 2019),甚至影响至遵义地区(Yan Hao et al., 2020)。安徽巢湖二叠系孤峰组硅质岩中也发现有热液硅的输入,且与硅质岩共生有多层火山灰层(杨水源等, 2008)。可见,峨眉地幔柱早期海底火山活动影响范围很广、程度很深。赵振洋等(2020)进一步对中下扬子区北缘中二叠统孤峰组硅质岩开展综合研究,推断峨眉地幔柱早期海底火山活动是形成区内热水成因硅质岩的重要基础,这一推论暗示峨眉地幔柱早期海底火山活动很可能对区域同时期热水沉积硅质岩具有重要控制和影响。峨眉山玄武岩沉积序列中夹层灰岩偏低的锶同位素组成(0.7068~0.7070)也被认为与当时强烈的火山活动有一定关系(Huang Hu et al., 2019)。此外,贵州遵义二叠纪锰矿床赋矿硅质岩的 $n(^{87}Sr)/n(^{86}Sr)$ 值介于 0.706860~0.706866(徐海, 2022),结合沉积学、精细岩相学研究,也认为硅质岩的形成可能受到峨眉地幔柱早期水下火山活动影响。遵义二叠纪硅质岩硅同位素研究也发现了热液硅的明显参与(叶远谋等, 2020)。另从不同成因硅质岩的时空分布来看,扬子板块中西部二叠纪硅质岩受热水活动影响似乎更为显著(杨海生等, 2003; 邱振等, 2010, 2011; 刘志臣等, 2013; 徐海等, 2017),而中东部地区同层位硅质岩记录的热水活动信息相对较弱(杨水源等, 2008; 孙秀凤等, 2016; 谈昕等, 2018; 赵振洋等, 2020)。

上文分析已表明,元素地球化学证据集中指示纳雍营盘硅质岩为热水沉积成因。另从其产出特征、形成时代等方面综合分析,该硅质岩主要产于峨眉山高钛玄武岩之下,表明其形成时间应早于峨眉山玄武岩大规模溢流时间。同时,纳雍营盘硅质岩与黔北二叠纪锰矿底板硅质岩具有等时性,并可与中下扬子区中二叠统孤峰组热水成因硅质岩(赵振洋等, 2020)进行对比。Yan Hao 等(2020)对遵义锰矿顶底板粘土岩中锆石开展 U-Pb 定年,结果为 261.6±2.4 Ma 和 262.5±2.3 Ma,这一结果较好地对应于峨眉地幔柱早期海底火山活动时间(孙亚东, 2013)。此外,结合朱江(2019)关于峨眉地幔柱早期(水下)火山活动方式、影响范围等综合调查研究成果,纳雍营盘剖面位于此次火山活动影响范围之内。因此,我们认为,纳雍营盘硅质岩的形成与峨眉地幔柱早期海底火山活动密切相关,这一时期强烈的海底火山活动及与之相关的热水/液作用为包

括纳雍营盘在内的广大区域硅质沉积提供了重要物源,是区域热水成因硅质岩形成的重要基础。此外,这一结果也从一个侧面,为限定滇东至黔北二叠纪锰矿床物质来源,约束矿床成因提供了新的科学证据。

5 结论

(1)贵州纳雍营盘二叠纪硅质岩 Al/(Al+Fe+Mn)、Al—Fe—Mn、Fe—Mn—(Cu+Ni+Co)和 U—Th 等成因判别图解集中显示,硅质岩形成过程中有明显的热水物质参与,硅主要来自于热水体系。结合硅质岩 Ce/Ce^{*}、$(La/Ce)_{N}$ 值及古地理特征,认为纳雍营盘硅质岩沉积环境为同沉积断裂的深水相的黔中台沟。

(2)峨眉地幔柱早期海底火山活动或与之相关的热水/液作用提供了纳雍营盘硅质岩沉积所需的硅质组分,区域内同沉积断裂及拉伸作用形成了较深水黔中台沟,两者共同控制和约束区域硅质岩的形成和时空分布。

(3)峨眉地幔柱早期海底火山活动影响范围广、程度深,综合华南地区二叠纪硅质岩时空分布规律和成因,认为峨眉地幔柱早期海底火山活动可能对华南二叠纪硅质岩有重要控制作用。

致谢:谨以此文祝贺杨文采主编 80 华诞! 广州澳实分析检测中心以及中国科学院地球化学研究所矿床学地球化学国家重点实验室为本文样品测试分析提供了支持和帮助,在论文撰写过程中得到了课题组老师的悉心指导,在此致以诚挚的谢意。

参 考 文 献 / References

(The literature whose publishing year followed by a "&" is in Chinese with English abstract; The literature whose publishing year followed by a "#" is in Chinese without English abstract)

陈文一, 刘家仁, 王中刚, 郑启钤. 2003. 贵州峨眉山玄武岩喷发期的岩相古地理研究. 古地理学报, 5(1): 17~28.

何斌,徐义刚,肖龙,王雅玫,王康明,沙绍礼. 2006. 峨眉山地幔柱上升的沉积响应及其地质意义. 地质论评,52(1):30~37.

加娜提古丽·吾斯曼, 周瑶琪, 姚旭, 许汉华, 方雪. 2017. 安徽省巢湖地区二叠纪栖霞组、孤峰组硅质岩地球化学特征对比及大地构造背景分析. 现代地质, 31(4): 734~745.

江冉, 付勇, 徐志刚, 裴浩翔, 王富良, 周文喜. 2016. 二叠纪茅口晚期锰矿成矿作用的地球化学约束——以遵义市南茶锰矿为例. 沉积学报, 34(6): 1032~1043.

林良彪, 陈洪德, 朱利东. 2010. 川东茅口组硅质岩地球化学特征及成因. 地质学报, 84(4): 500~507.

刘平, 廖友常, 殷科华, 叶德书, 朱华, 韩忠华, 杨光龙. 2008. 与火山活动有关的热水沉积锰矿——以贵州二叠纪锰矿为例. 中国地质, 35(5): 992~1006.

刘志臣, 张远国, 陈登, 刘金海, 崔忠强, 胡乐宇, 钟月丽. 2013. 贵州遵义锰矿区"白泥塘层"硅质岩地球化学特征及其地质意义. 矿物学报, 33(4): 665~670.

邱振, 王清晨. 2010. 湘黔桂地区中上二叠统硅质岩的地球化学特征及沉积背景. 岩石学报, 26(12): 3612~3628.

邱振, 王清晨, 严德天. 2011. 广西来宾蓬莱滩剖面中上二叠统硅质岩的地球化学特征及沉积背景. 岩石学报, 27(10): 3141~3155.

孙秀凤, 王国庆. 2016. 鄂西二叠系孤峰组层状硅质岩及硅质结核成因. 铀矿地质, 32(1): 23~30.

孙亚东. 2013. 华南古—中生代之交火山作用的古气候影响和生物多样性响应. 导师:赖旭龙, Wignall P, Joachimski M. 武汉: 中国地质大学(武汉)博士学位论文: 1~134.

谈昕, 邱振, 卢斌, 董大忠, 施振生, 陈留勤, 江增光. 2018. 华南地区不同时代硅质岩地球化学特征及地质意义. 科学技术与工程, 18(2): 7~19.

王忠诚, 吴浩若, 邝国敦. 1995. 广西晚古生代硅岩的地球化学及其形成的大地构造环境. 岩石学报, 11(4): 449~455.

夏邦栋, 钟立荣. 1995. 下扬子区早二叠世孤峰组层状硅质岩成因. 地质学报, 69(2): 125~137.

徐海, 高军波, 杨瑞东, 郑禄林, 张旭. 2017. 贵州遵义二叠系锰矿区硅质岩成因及成矿意义. 地质科学, 52(4): 1297~1311.

徐海. 2022. 华南黔北—滇东二叠纪锰矿成矿物质来源及成矿机制研究. 导师:高军波. 贵阳: 贵州大学博士学位论文: 1~160.

徐义刚, 王焰, 位荀, 何斌. 2013a. 与地幔柱有关的成矿作用及其主控因素. 岩石学报, 29(10): 3307~3322.

徐义刚, 何斌, 罗震宇, 刘海泉. 2013b. 我国大火成岩省和地幔柱研究进展与展望. 矿物岩石地球化学通报, 32(1): 25~39.

颜佳新, 赵坤. 2002. 二叠~三叠纪东特提斯地区古地理、古气候和古海洋演化与地球表层多圈层事件耦合. 中国科学: 地球科学, 32(9): 751~759.

杨海生, 周永章, 杨志军, 张澄博, 杨小强. 2003. 热水沉积硅质岩地球化学特征及意义——以华南地区为例. 中山大学学报: 自然科学版, 42(6): 111~115.

杨水源, 姚静. 2008. 安徽巢湖平顶山中二叠统孤峰组硅质岩的地球化学特征及成因. 高校地质学报, 14(1): 39~48.

杨玉卿, 冯增昭. 1997. 华南下二叠统层状硅岩的形成及意义. 岩石学报, 13(1): 111~120.

叶远谋, 付勇, 江冉, 谯文浪, 龙宣霖. 2020. 黔北瓜德鲁普世—乐平世转换时期大规模成硅事件硅质来源厘定. 地球学报, 41(5): 699~713.

张成江,汪云亮,侯增谦. 1999. 峨眉山玄武岩系的 Th、Ta、Hf 特征及岩浆源区大地构造环境探讨. 地质论评,45(7): 858~860.

张聪, 黄虎, 侯明才. 2017. 地球化学方法在硅质岩成因与构造背景研究中的进展及问题. 成都理工大学学报(自然科学版), 44(3): 293~304.

赵振洋, 李双建, 王根厚. 2020. 中下扬子北缘中二叠统孤峰组层状硅质岩沉积环境、成因及硅质来源探讨. 地球科学进展, 35(2): 137~153.

周永章, 何俊国, 杨志军, 付伟, 杨小强, 张澄博, 杨海生. 2004. 华南热水沉积硅质岩建造及其成矿效应. 地学前缘, 11(2): 373~377.

朱江. 2019. 峨眉山大火成岩省地幔柱动力学及其环境效应研究. 导师: 张招崇. 北京: 中国地质大学(北京)博士学位论文: 1~163.

Adachi M, Yamamoto K, Sugisaki R. 1986. Hydrothermal chert and associated siliceous rocks from the northern Pacific their geological significance as indication of ocean ridge activity. Sedimentary Geology, 47(1~2): 125~148.

Boström K, Peterson M. 1969. The origin of aluminum-poor ferromanganoan sediments in areas of high heat flow on the East

Pacific Rise. Marine Geology, 7(5): 427~447.

Boström K. 1983. Genesis of ferromanganese deposits-diagnostic criteria for recent and old deposits. Hydrothermal Processes at Seafloor Spreading Centers. Springer US: 473~489.

Chen Wenyi, Liu Jiaren, Wang Zhonggang, Zheng Qiqian. 2003&. Study on lithofacies palaeogeography during the permian emeishan basalt explosion in Guizhou province. Journal of Paleogeography, 5(1): 17~28.

Gao Yongbao, Teng Jiaxin, Li Wenyuan, Chen Denghui, Sui Qinglin, Jing Delong, He Yongkang, Bai Jianke. 2018. Geology, geochemistry and ore genesis of the Aoertuokanashi manganese deposit, western Kunlun, Xinjiang, Northwest China. Acta Petrologica Sinica, 34(8): 2341~2358.

He Bin, Xu Yigang, Chung Sunling, Xiao Long, Wang Yamei. 2003. Sedimentary evidence for a rapid, kilometer-scale crustal doming prior to the eruption of the Emeishan flood basalts. Earth and Planetary Science Letters, 213(3~4): 389~403.

He Bin, Xu Yigang, Xiao Long, Wang Yamei, Wang Kangming, Sha Shaoli. 2006&. Sedimentary responses to uplift of Emeishan Mantle Plume and its implications. Geological Review, 52(1): 30~37.

He Bin, Xu Yigang, Huang Xiaolong, Luo Zhenyu, Shi Yuruo Yang Qijun, Yu Songyue. 2007. Age and duration of the Emeishan flood volcanism, SW China: Geochemistry and SHRIMP zircon U-Pb dating of silicic ignimbrites, post-volcanic Xuanwei Formation and clay tuff at the Chaotian section. Earth and Planetary Science Letters, 255: 306~323.

Hou Zengqian, Lu Jiren, Lin Shengzhong. 2006. Heterogeneity of a plume axis: bulk-rock geochemical evidence from picrites and basalts in the Emei large igneous province, southwest China. International Geology Review, 48: 1087~1112.

Huang Hu, Hou Mingcai, Qing Hairuo, Zhou Lian, Yang Jianghai, Du Yuansheng, Jingchun Tian, Ni Shijun, Xiong Fuhao. 2019. The contribution of the Emeishan large igneous province to the strontium isotope evolution of the Capitanian seawater. International Geology Review, 61(15): 1927~1939.

Jianatiguli Wusiman, Zhou Yaoqi, Yao Xu, Xu Hanhua, Fang Xue. 2017&. Geochemical characteristics comparison and tectonic background analysis of siliceous rocks from Qixia Formation and Gufeng Formation of Permian in Chaohu area, Anhui Province. Geoscience, 31(4): 734~745.

Jiang Ran, Fu Yong, Xu Zhigang, Pei Haoxiang, Wang Fuliang, Zhou Wenxi. 2016&. Geochemical constraints on the manganese mineralization during the Latest Maokou Epoch of Permian—Example from the Nancha manganese ore deposit in Zunyi city, northern Guizhou. Acta Sedimentologica Sinica, 34(6): 1032~1043.

Kametaka M, Takebe M, Nagai H, Zhu S, Takayanagi Y. 2005. Sedimentary environments of the Middle Permian phosphorite—chert complex from the northeastern Yangtze platform, China; the Gufeng Formation: A continental shelf radiolarian chert. Sedimentary Geology, 174(3~4): 197~222.

Lin Liangbiao, Chen Hongde, Zhu Lidong. 2010&. The origin and geochemical characteristics of Maokou Formation silicalites in the eastern Sichuan basin. Acta Ceologica Sinica, 84(4): 500~507.

Liu Ping, Liao Youchang, Yin Kehua, Ye Deshu, Zhu Hua, Han Zhonghua, Yang Guanglong, 2008&. Hydrothermal sedimentary manganese deposits associated to volcanic activities—Permian manganese deposit in Guizhou. Geology of China, 35(5): 992~1006.

Liu Zhichen, Zhang Yuanguo, Chen Deng, Liu Jinhai, Cui Zhongqiang, Hu Leyu, Zhong Yueli. 2013&. Geochemical characteristics and geological significance of "Bainitangceng" siliceous rocks in Zunyi manganese ore fields, Guizhou Province, China. Acta Mieralogica Sinica, 33(4): 665~670.

Mclennan S M. 1989. Rare earth elements in sedimentary rocks: Influence of provenance and sedimentary processes. Reviews in Mineralogy and Geochemistry, 21(1): 169~200.

Montañez I P, Poulsen C J. 2013. The Late Paleozoic ice age: An evolving paradigm. Annual Review of Earth and Planetary Sciences, 41(1): 629~656.

Murchey B L, Jones D L. 1992. A mid-Permian chert event: widespread deposition of biogenic siliceous sediments in coastal, island arc and oceanic basins. Palaeogeography Palaeoclimatology Palaeoecology, 96(1): 161~174.

Murray R W, Brink M R B T, Gerlach D C, Iii G P R, Jones D L. 1991. Rare earth, major, and trace elements in chert from the Franciscancomplex and Monterey group, Californian: Assessing REE sources to fine-grained marine sediments. Geochim. Cosmochim. Acta, 55: 1875~1895.

Murray R W. 1994. Chemical criteria to identify the depositional environment of chert: general principles and applications. Sedimentary Geology, 90(3~4): 213~232.

Nozaki Y, Zhang J, Amakawa H. 1997. The fractionation between Y and Ho in the marine environment. Earth and Planetary science Letters, 148: 329~340.

Qi Liang, Gregoire D C. 2000. Determination of trace elements in twenty six Chinese geochemistry reference materials by inductively coupled plasma-mass spectrometry. Geostandards Newsletter, 24(1): 51~63.

Qie Wenkun, Algeo T J, Luo Genming, Herrmann A. 2019. Global events of the Late Paleozoic (Early Devonian to Middle Permian): A review. Palaeogeography, Palaeoclimatology, Palaeoecology, 531: 109259.

Qiu Zhen, Wang Qingchen, Yan Detian. 2011&. Geochemistry and sedimentary background of the Middle—Upper Permian cherts in the Penglaitan section, Laibin, Guangxi Province. Acta Petrologica Sinica, 27(10): 3141~3155.

Qiu Zhen, Wang Qingchen. 2010&. Geochemistry and sedimentary background of the Middle—Upper permian cherts in the Xiang—Qian—Gui region. Acta Petrologica Sinica, 26(12): 3612~3628.

Shellnutt J G, Wang C Y, Zhou M F, Yang Y. 2009. Zircon Lu - Hf isotopic compositions of metaluminous and peralkaline A-type granitic plutons of the Emeishan large igneous province (SW China): Constraints on the mantle source. Journal of Asian Earth Sciences, 35(1): 45~55.

Shellnutt J G, Pham T T, Denyszyn S W, Yeh M W, Tran T A. 2020. Magmatic duration of the Emeishan large igneous province: Insight from northern Vietnam. Geology, 48(5). doi: 10.1130/G47076.1.

Sun Xiufeng, Wang Guoqing, 2016&. Genesis of stratified siliceous rocks and concretion of Permian Gufeng Formation in Western Hubei. Uranium Geology, 32(1): 23~30.

Sun Yadong, Lai Xulong, Wignall P B, Widdowson M, Ali J R, Jiang Haishui, Wang Wei, Yan Chunbo, Bond D P G, Védrine S. 2010. Dating the onset and nature of the Middle Pemmian Emeishan large igneous province eruptions in sw China using conodont biostratigraphy and its bearing on mantleplume uplift models. Lithos, 119(1~2): 20~33.

Sun Yadong. 2013&. Coupling climatic and biodiversity changes with volcanisms during the Palaeozoic—Mesozoic upheavals in South

China. Tutor: Lai Xulong, Paul Wignall, Michael Joachimski. Wuhan: Doctoral dissertation of China University of Geosciences (Wuhan): 1~134.

Tan Xin, Qiu Zhen, Lu Bin, Dong Dazhong, Shi Zhensheng, Chen Liuqin, Jiang Zengguang. 2018&. Geochemical characteristics for siliceous rocks of different ages in South China and their geological significance. Science, Technology and Engineering, 18(2): 7~19.

Ukstins-Peate I, Bryan S E. 2008. Re-evaluating plume-induced uplift in the Emeishan Large Igneous Province. Nature Geoscience, 1(9): 625~629.

Wang Zhongcheng, W Haoruo, Kuang Guodun. 1995&. Geochemistry and origin of Late Paleozoic cherts in Guangxi and their explanation of tectonic environments. Acta Petrologica Sinica, 11(4): 449~455.

Wei Hengye, Wei Xuemei, Qiu Zhen, Song Huyue, Shi Guo. 2016. Redox conditions across the G—L boundary in South China: evidence from pyrite morphology and sulfur isotopic compositions. Chemical Geology, 440: 1~14.

Wignall P B, Sun Y D, Bond DP G, Izon G, Newton R J, Vedrine S, Widdowson M, Ali J R, Lai X, Jiang H. 2009. Volcanisn, mass eztinction, and carbon isotope fluctuations in the Middle Permian of China. Science, 342(29): 1179~1182.

Wonder J D, Spry P G, Windom K E. 1988. Geochemistry and origin of manganese-rich rocks related to iron-formation and sulfide deposits, western Georgia. Economic Geology, 83(5): 1070~1081.

Wu Qiong, Ramezani J, Zhang Hua, Yuan Dongxun, Erwine D H, Henderson C M, Lambert L L, Zhang Yichun, Shen Shuzhong. 2020. High-precision U-Pb zircon age constraints on the Guadalupian in West Texas, USA. Palaeogeography Palaeoclimatology Palaeoecology, 548: 109668.

Xia Bangdong, Zhong Lirong. 1995&. The origin of cherts of the early Permian Gufeng formation in the lower Yangtze area, eastern china. Acta Geologica Sinica, 69(2): 125~137.

Xu Hai, Gao Junbo, Yang Ruidong, Feng Kangning, Wang Longbo, Chen Jun. 2021. Metallogenic mechanism of large manganese deposits from permian manganese ore belt in western South China Block: new mineralogical and geochemical evidence. Ore Geology Reviews. 132 (1~2): 103993.

Xu Hai, Gao Junbo, Yang Ruidong, Zheng Lulin, Zhang Xu. The early Permian siliciclastic rocks in the Lower Yangzi. 2017&. The origin of siliceous rocks in Zunyi Permian manganese ore fields in Guizhou Province and their metallogenic significance. Scientia Geologica Sinica , 52(4): 1297~1311.

Xu Hai. 2022&. Ore-forming material sources and metallogenic mechanism of Permian manganese deposits in northern Guizhou and eastern Yunnan, Tutor: Gao Junbo. Guiyang: Doctoral dissertation of Guizhou University: 1~160.

Xu Yigang, Chung Sunling, Jahn B M, Wu Genyao. 2001. Petrologic and geochemical constraints on the petrogenesis of Permian—Triassic Emeishan flood basalts in southwestern China. Lithos, 58: 145~168.

Xu Yigang, He Bin, Luo Zhenyu, Liu Haizhuan. 2013b&. Study on mantle plume and large igneous provinces in China: An overview and perspectives. Bulletin of Mineralogy, Petrology and Geochemistry, 32(1): 25~39.

Xu Yigang, Wang Yan, Xun Wei, He Bin. 2013a&. Mantle plume-related mineralization and their principal controlling factors. Acta Petrologica Sinica, 29(10): 3307~3322.

Yamamoto K. 1987. Geochemical characteristics and depositional environments of cherts and associated rocks in the Franciscan and Shimanto Terranes. Sedimentary Geology, 52(1~2): 65~108.

Yan Hao, Pi Daohui, Jiang Shaoyong, Hao Weiduo, Mänd K, Robbins L J, Li Long, Konhauser K O. 2020. New constraints on the onset age of the Emeishan LIP volcanism and implications for the Guadalupian mass extinction. Lithos, 360~361: 1~14.

Yan Jiaxin, Zhao Kun. 2002#. Permian—Triassic paleogeography, paleoclimate and paleo-oceanic evolution of the Eastern Tethys coupled with geosurface multispheric events. Scientia Sinica (Terrae), 32(9): 751~759.

Yang Haisheng, Zhou Yongzhang, Yang Zhijun, Zhang Chengbo, Yang Xiaoqiang. 2003&. Geochemical characteristics and significance of hlydrothermal cherts——A case study of South China. Acta Scientiarum Naturalium Universitatis Sunyatseni, 42(6):111~115.

Yang Shuiyuan, Yao Jing. 2008&. Geochemistry and origin of siliceous rocks from the Gufeng Formation of Middle Permian in the Pingdingshan area, Chaohu Region, Anhui Province. Geological Journal of China Universities, 14(1): 39~48.

Yang Yuqing, Feng Zengzhao. 1997&. Formation and significance of the bedded siliceous rocks of the Lower Permian in South China. Acta Petrologica Sinica, 13(1): 111~120.

Ye Yuanmou, Fu Yong, Jiang Ran, Qiao Wenlang, Long Xuanlin. 2020&. The determination of silicon source of large-scale chert events during the Permian Guadalupian—Lepingian Transition Period in northern Guizhou Provincoe. Acta Geoscientica Sinica, 41(5): 699~713.

Zhang Chengjiang, Wang Yunliang, Hou Zengqian. 1999&. Th, Ta and Hf characteristics and the tectonic setting of magmatic source region of Emeishan Basalts. Geological Review, 45(7): 858~860.

Zhang Cong, Huang Hu, Hou Mingcai. 2017&. Progress and problems in the geochemical study on chert genesis for interpretation of tectonic background. Journal of Chengdu University of Technology (Science of Technology Edition), 44(3): 293~304.

Zhao Zhenyang, Li Shuangjian, Wang Genhou. 2020&. Discussion on sedimentary environments, origin and source of Middle Permian Gufeng Formation bedded cherts in the northern margin of the Middle—Lower Yangtze area. Advances In Earth Science, 35(2): 137~153.

Zhong Hong, Zhu Weiguang, Hu Ruihzong, Xie Liewen, He Defeng, Liu Feng, Chu Zhuyin. 2009. Zircon U-Pb age and Sr—Nd—Hf isotope geochemistry of the Panzhihua A-type syenitic intrusion in the Emeishan large igneous province, southwest China and implications for growth of juvenile crust. Lithos, 110: 109~128.

Zhong Hong, Campbell I H , Zhu Weiguang, Allen C M, Hu Ruizhong, Xie Liewen, He Defeng. 2011. Timing and source constraints on the relationship between mafic and felsic intrusions in the Emeishan large igneous province. Geochimica et Cosmochimica Acta, 75(5): 1374~1395.

Zhong Yuting, Mundil R, Chen Jun, Yuan Dongxun, Denyszyn S W, Jost A B, Payne J L, He Bin, Shen Shuzhong, Xu Yigang. 2020. Geochemical, biostratigraphic, and high-resolution geochronological constraints on the waning stage of Emeishan Large Igneous Province. Geological Society of America Bulletin, 132(9~10): 1969~1986.

Zhou Meifu, Malpas J, Song Xieyan, Robinson R T, Sun Min, Kennedy A K, Lesher C M, Keays R R. 2002. A temporal link between the Emeishan large igneous province (SW China) and the end—Guadalupian mass extinction. Earth and Planetary Science Letters, 196: 113~122.

Zhou Yongzhang, He Junguo, Yang Zhijun, Fu Wei, Yang Xiaoqiang, Zhang Chengbo, Yang Haisheng. 2004&. Hydrothermally

sedimentary formations and Related mineralization in south china. Earth Science Frontiers, 11(2): 373~377.

Zhu Jiang. 2019&. A study of mantle plume dynamics and its environmental effect in the Emeishan Large Igneous Province. Tutor: Zhang Zhaocong. Beijing: Doctoral dissertation of China University of Geosciences (Beijing): 1~163.

The genesis and geological significance of the siliciclastic rocks of the Middle Permian Maokou Formation at Yingpan, Nayong, Guizhou

YANG Guiyuan[1, 2)], GAO Junbo[1, 2)], YANG Ruidong[1, 2)], LIU Zhichen[3)], XU Hai[4)]

1) *College of Resource and Environment Engineering, Guizhou University, Guiyang*, 550025;

2) *Key Laboratory of Karst Geological Resources and Environment, Ministry of Education, Guizhou University, Guiyang*, 550025;

3) *The* 102 *Geological Brigade, Guizhou Bureau of Geological and Mineral Exploration and Development, Zunyi, Guizhou*, 563003;

4) *Department of Tourism and Geography, Tongren University, Tongren, Guizhou*, 554300

Objectives: The siliciclastic rocks of the Middle Permian Maokou Formation at Yingpan, Nayong, Guizhou, are the main object of this study, focusing on the genesis of siliciclastic rocks and the origin of defined silica using elemental earth methods.

Methods: Based on the field investigation work, the ratio characteristics and enrichment patterns of major, trace and rare earth elements were analyzed by elemental geochemical methods, combined with geological background and petrographic paleogeographic features to discern the siliciclastic genesis and depositional environment.

Results: Elemental geochemical correlation ratios and diagrams of diagenetic discrimination indicate that there was a significant input of hot water material during the formation process, and silicon was mainly derived from the hot water system. The depositional environment is the Qianzhong Terrace Trench in the deep-water phase of the same sedimentary fracture.

Conclusions: The early submarine volcanism of the Emei mantle column or the associated hot water action provided the siliceous fraction required for the deposition of siliciclastic rocks at Yingpan, Nayong. And the early submarine volcanism of the Emei mantle column may have an important controlling role on the Permian siliciclastic sedimentation in South China.

Keywords: diagenesis; siliciclastic rocks; Permian; Yingspan, Nayong, Guizhou

Acknowledgements: This work was supported by the National Natural Science Foundation of China (Nos. 42163006, 41890841, U1812402), Guizhou Scientific and Technological Innovation Talent Team Project of Sedimentary Deposits (No. Guizhou Science and Technology Cooperation Platform Talent [2018]5613), Guizhou Talent Base Project (No. RCJD2018-21) and Guizhou Graduate Research Fund Project (No. Guizhou Jiaohe YJSCXJH[2020]181). Thanks to Guangzhou Aoshi Analysis and Testing Center and State Key Laboratory of Mineral Deposit Geochemistry, Institute of Geochemistry, Chinese Academy of Sciences for their support and help in the sample testing and analysis of this paper, and thanks to the teachers of the research group for their careful guidance

First author: YANG Guiyuan, female, born in 1997, master degree, is maily engaged in the study of sedimentary deposits; Email: yangguiyuan_08@163. com

Corresponding author: GAO Junbo, male, born in 1985, professor, Ph. D., supervisor, is mainly engaged in the study of mineral deposit geology and geochemistry; Email: gaojunbo1985@ 126. com

Manuscript received on: 2022-03-21; Accepted on: 2022-06-22; Network published on: 2022-07-20

Doi: 10. 16509/j. georeview. 2022. 07. 031　　**Edited by**: LIU Zhiqiang